Performance Modelling Of Flap-Type Wave Energy Converter Array Flaps With Various Dynamic Characteristics

Saeidtehrani, S.; Lavidas, G.

Publication date
2022

Document Version
Final published version

Published in
Proceedings of the ASME 2022 41st International Conference on Ocean, Offshore and Arctic Engineering

Proceedings of the ASME 2022 41st International Conference on Ocean, Offshore and Arctic Engineering
OMAE2022
June 5-10, 2022, Hamburg, Germany

OMAE2022-79869

PERFORMANCE MODELLING OF FLAP-TYPE WAVE ENERGY CONVERTER ARRAY: FLAPS WITH VARIOUS DYNAMIC CHARACTERISTICS

Saghy Saeidtehrani
Delft University of Technology (TU Delft) Delft, Netherlands

George Lavidas
Delft University of Technology (TU Delft) Delft, Netherlands

ABSTRACT

Generally, it is expected that the total power of N energy converters in an array will be less than N times the power of a single operative converter. The goal of this paper is to enhance the oscillation of the flap-type WEC and consequently the energy extraction of the whole array in front of a coastal structure. Flaps in an array show different response patterns in terms of amplitude and frequency based on their dynamic characteristics, incoming wave frequencies, and the distance between the WECs. Through this work, different dynamic characteristics for each flap in combination with various distances between proximate flaps are investigated. An experimentally validated numerical model developed for the simulation of flap-type WEC operating as single and in an array is used for the simulation. The effects of dynamic characteristics and WEC distances on the response and power production are estimated and discussed in detail for a flap operating in an array of two and five. It is shown that by changing the distance between two flaps, the response is enhanced up to 20%. The findings suggest the most efficient ratio of dynamic characteristics of flaps in an array of two is having a period half to the incoming wave period. However, for an array of five, having staggered flaps with a period equal to the incoming wave period make a 4% increase in the overall response of each flap.

Keywords: Flap-type WEC; Dynamic characteristics; Performance modeling; Distance of WECs in an array

NOMENCLATURE

C_F	Mechanical damping
C_D	Drag coefficient
C_P	PTO damping
d	Water depth
g	Gravity acceleration
H	Wave height
θ	Flap rotation
I	Moment of inertia
I^A	Second moment
I^V	First moment
h_r	Coordinate of the centre of rotation
k	Wave number
K_H	Hydrostatic stiffness
K_P	PTO stiffness
M	Mass of a floating body
n	Unit normal vector pointing into the body
ρ	Water density
u	Velocity
φ	Fluid flow velocity potential

1. INTRODUCTION

Looking to the future is developing farms of WECs to increase energy extraction [1]. However, it is generally accepted that the total power absorbed from a resource by n number of energy converters is less than n times of an isolated device [2].

This subject for WECs is more challenging and uncertain due to the absorption, radiation, and diffraction of waves from multiple WEC bodies in the farm [3]. These wave-structure effects caused by the WEC operation in an array could influence the power absorbance [4] which emerges studies on layout optimization [5]–[7].

Studies show that the array arrangement optimization and control systems for point absorber WECs can lead to an increase of power efficiency up to 15 % [8].

It should be no surprise that the diversity of WEC concepts shows various destructive or constructive effects of WECs in a farm [7], [9], [10]. Therefore, there is no specific layout scheme that the whole industry can settle for it.

More importantly, any proposed scheme for the optimization should be considered with uncertainty and possible

room for adaptation to the WEC concept and its peculiar interaction with fluid and other WECs around.

The main question is can the dynamic characteristics and distance of WECs be tuned in a way that a minimum steady level of power in an array is guaranteed?

This paper is focused to respond this question for a flap WEC mounted on a breakwater. It should be pointed out that the confined and reflected water between flaps and breakwater significantly affects the flaps' behavior which is a very useful idea for benefiting from the already existent nearshore or developing multipurpose structures [11], [12].

Through this paper, first, general information on the WEC concept, the methodology, and the mathematical description for the WEC simulation is presented.

Then a combined algorithm of the numerical solver and the parametric study of the distance between the flaps in an array of two is presented to estimate the response and power of flaps (Section 3.1). Section 3.2 and 3.3 examine the flap's behavior in an array of two and five flaps when they have different dynamic characteristics.

The findings of this paper lead to suggestions on the layout, the distance of flaps, and the dynamic characteristics of each flap in an array to enhance the overall energy extraction.

2. WEC CONCEPT AND MATHEMATICAL BACKGROUND

This study uses the experimentally validated numerical model developed for simulating the Flap-type WEC in an array mounted on a breakwater.

The primary proposed concept encompassed five Flap-type WECs hinged to the seaward horizontal surface of a vertical breakwater [13], [14]. **Figure 1** shows the 1:40 scale model of the breakwater and the flaps mounted on the seawall.

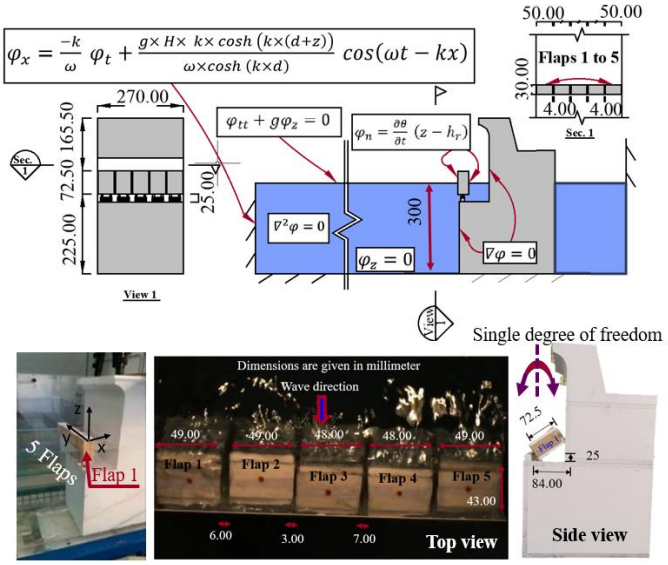

Figure 1: WEC CONCEPT- THE MATHEMATICAL DESCRIPTION OF THE DOMAIN BOUNDARIES (TOP), EXEMPLARY PICTURES OF EXPERIMENTAL TEST (BOTTOM)

Figure 1- Top shows the drawing of the WEC concept and the breakwater, along with the boundary conditions in xz plane. The sidewalls of the flume in the experimental tests are simulated as walls in 3D numerical model.

Figure 1- Bottom represents some experimental test pictures. Dimensions are also presented for both experimental pictures and numerical schematic views.

The dynamic motion of the flap is simulated by the idealized model with a single degree of freedom [15], [16]; this model is further developed to consider the mechanical damping, PTO, and drag effects [17], [18]:

$$I\ddot{\theta} + K_H\theta + K_P\theta + C_P\dot{\theta} + C_F\theta + C_{D1}\dot{\theta}|\dot{\theta}|(\theta \geq 1) + C_{D2}\dot{\theta}|\dot{\theta}|(\theta < 1) = -\rho\int_s \varphi_t(z - h_r)\,ds \quad (1)$$

The moment of inertia and hydrostatic stiffness proportional to acceleration ($\ddot{\theta}$) and rotation (θ) are represented by I and K_H and are analytically calculated. The moment of inertia for pitch motion is the summation of the second moment of inertia on two perpendicular axes to the axes of rotation (y as shown in **Figure 1**- Bottom)**.** The hydrostatic stiffness is also calculated by the following formula [15]:

$$I = \rho g(I^A_{xx} + I^V_z) - Mg\,(z^c - Z^0) \quad (2)$$

g is the gravity acceleration; M is the mass; I^V_z and I^A_{xx} are the first moment around plane $z = Z^0$ and the second moment around x, respectively; z^c is the center of rotation; and Z^0 is the Z coordinate at rest position. Further details on the calculation of stiffness and mass matrix for the floating body can be found in [15].

From the previous study, the mass is set to make the flap natural period almost half of the average incoming wave period and the distance from the breakwater was set to amplify the response to the incoming wave [18]. Therefore, the corresponding moment of inertia and hydrostatic stiffness is analytically estimated as $9.86 \times 10 - 5\ [kgm^2]$ and $0.028\ [\frac{kgm^2}{s^2}]$, respectively.

The Power-Take-Off (PTO) is simulated by using two terms corresponding to damping and stiffness and represented by stiffness and damping coefficient K_P and C_P. The process for the optimization of the PTO coefficients based on the flap dynamic characteristics is fully described in [18].

Mechanical damping (C_F) is estimated as $1.2 \times 10^{-4}\ kgm^2/s$ based on the free oscillation dry tests [9]. In the previous hybrid experimental and numerical study was shown that the drag coefficient is amplitude-dependent; therefore, two coefficients for darg are introduced which depend on the amplitude of the oscillation [9], [17], [18]. Drag coefficient (C_D) by the values of $2.07 \times 10^{-3}\ kgm^2$ for amplitude higher than 1

radian and $2.07 \times 10^{-4}\, kgm^2$ for oscillation with lower amplitude than 1 are considered for the analyses.

φ represents fluid flow velocity potential and φ with subscripts shows the time or spatial derivative of that. The dynamic pressure on the body is stimulated by the right-hand side of the equation and integrates over the submerged floating body (s) at rest position. ρ is the density of water; and h_r is the z coordinate of the centre of rotation.

The radiation, diffraction, and incident potential problems are solved simultaneously by solving the Laplace equation with appropriate boundary conditions [19].

For the simulation, the 3D domain is used in which the dynamic equation of each flap is connected to the fluid flow equations by means of boundary conditions (see Figure 1- Top, boundary conditions). Equation (1) connects the flap motion to the pressure induced by the fluid on the flap surface.

According to the number of flaps, the equations and the corresponding geometry and boundary conditions are defined. Therefore the model has enough flexibility to change the number, dynamic characteristics, and consequent distance between the flaps in the flume. Boundary conditions and dynamic equations of motions provide a two-way coupling between fluid and flaps [8], [17].

It should be noted that the hydrodynamic around the flaps which are more effective close to the natural frequency [20] is described by connecting the fluid velocity to the dynamic equation of flap.

Several sensitivity analyses for the mesh size and time step were conducted. Based on the results, an efficient time-stepping procedure with $\Delta t = 0.01\, s$ and the tolerance of $0.001\, s$ to control the internal time steps along with fine mesh with minimum element size equal to 1.2E-4 (m) are chosen for the analyses [9], [18].

This combination satisfies the Courant-Friedrichs-Lewy or CFL condition (u $\Delta t/\Delta x$), where u is the velocity, Δt, and Δx are the time step and the length interval [21].

The developed numerical model was experimentally validated for a flap operating as single and in an array of five flaps with three different sets of experimental tests including free oscillation dry tests, decay test in water, and response to wave action [9], [17].

Figure 2 shows the comparison of the experimental and numerical RMS of flap's response time series to wave action (For further details see [9], [17]).

The response is calculated for a scale model to the wave characteristics with $T_P \in [3.5\ 6.3]$ s and $H_s = 2$ m that has the maximum energy potential at the primary feasible site for the device [13].

The corresponding values for H_s and T_P would be 0.05 m and [0.6, 1] s. However, an extra range of the period [0.3, 1.1] for investigation on the flaps response to waves with the same and twice of the flaps' natural period is also considered for the validation of numerical simulation.

As it can be seen, in most of the cases, the response of all flaps in an array of five overlap each other. However, the out-of-phase responses can be observed in response to wave 0.3 s to 0.6 s due to the proximity of the wave period to the flaps' period [9], [17], [18]. For better representation, only the RMS response of flap 3 from numerical results are presented.

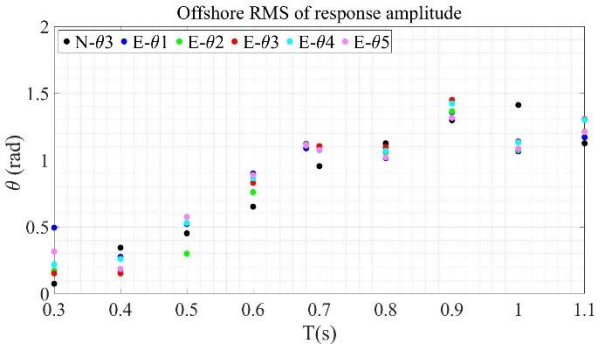

Figure 2: COMPARISON OF NUMERICAL (Nθ) AND EXPERIMENTAL RESULTS (Eθ) TO WAVE WITH SAME HEIGHT 0.05 m AND DIFFERENT PERIOD IN THE RANGE OF [0.3, 1.1] s

Here, the numerical model is used to study an array with flaps in different distances and dynamic characteristics in the same flume as will be explained in the following sections. Since the nonlinearities involved is characterized as nonlinear mathematical term dependent on the velocity of the flap (drag coefficient), it is expected that the model can fairly capture the flap responses' nonlinearities [22]–[24].

3. RESULTS AND DISCUSSION

This section provides an investigation on the flaps interaction at different distances from each other, and dynamic characteristics in an array. The response of the flaps to a representative wave with 2 m height and 4.9 s period (0.05 m, 0.78 s in scale model) are studied.

As was previously explained this wave height corresponds to the maximum energy potential in the power matrix of the proposed site the port of Piombino [13], [25]. The period is the average of the $T_P \in [3.5\ 6.3]$ s in the range of maximum energy potential [25].

Here, the same coefficients $K_P = 2.38 * 10^{-4}\, kgm^2/s^2$ and $C_P = 3.8 * 10^{-3}\, kgm^2/s$ for stiffness and damping from the previous study are utilized [18].

3.1 Parametric study of distance between two flaps in an array

The first part of the study deals with the distance of flaps with similar characteristics. The numerical solver is based on the mathematical model explained in Section 0, and is connected to parametric study to reflect the consequent changes in the pressure field around by the distance.

The distance of flaps is considered as a variable, and by developing a combined algorithm of the numerical solver and the parametric study; the distance between the flaps is changed.

For each distance, the equation of motion for wave-structure interaction is solved. As was previously explained in Section 2, the movement of the flaps is two-way connected to the fluid flow to be sure that the full interaction is captured. The first way, is by using the boundary condition on the flap surface which connects the movement of the flap with the movement of fluid particles (**Figure 1**).

The second connection is defined by using a function calculating the pressure at each time step and is introduced in the dynamic equation of flap motion, Equation (1).

For a farm of two flaps, there are two dynamic equations of motion, and two flaps in the numerical domain that are interacted with fluid around in each time step.

The minimum distance between the flaps is considered in such a way that there is only a small gap (8% of flap width) between two flaps, and for the maximum distance, each flap stands at the edge of the flume width (see **Figure 3**).

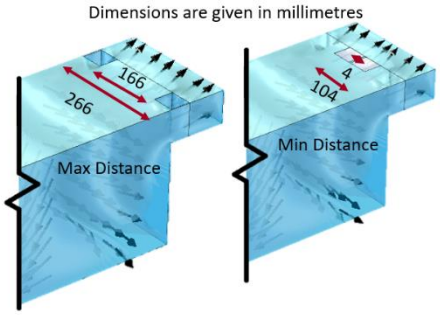

Figure 3: MIN AND MAX FLAP DISTANCES

In each loop, by changing the distance, the numerical domain between flaps is changed in terms of meshing and geometry. By changing the domain, the pressure on the flaps also changes, which is reflected in the equation of motion and partial differential equation simulating the fluid flow behavior.

The loop of the parametric study is set in a way, that each time, the distance increase by 30% of the flap width. The starting value is set to the minimum distance in which the flaps stand next to each other with the gap equal to 8% of flap width. The parameter GAP here is defined as non-dimensional scale of the flap's width.

In total, 11 cases have been studied, the exemplary results for the minimum, average, and maximum distance are provided in **Figure 4**.

Because of the symmetry, the time-series responses for both flaps are the same. The maximum response is obtained in the maximum distance. Interestingly, the response is lessened by decreasing the distance between the flaps.

Figure 5 shows the maximum and RMS response of flap for the total time series response and its relation with the gap between the two next flaps.

From **Figure 5**, a trend can be observed for the WEC flaps behavior; in fact, the relation between the distance and the maximum response is like a parabolic curve. By increasing the GAP between flaps to 3.3 times the flap width, the maximum

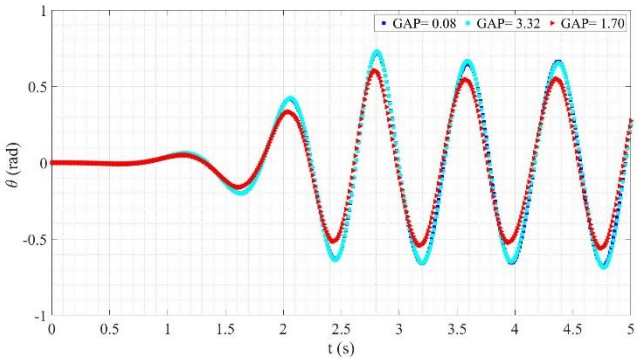

Figure 4: FLAP TIME SERIES RESPONSE FOR DISTANCE PARAMETRIC STUDY

response can be achieved. Although this response is only 1 % more than the maximum response when the flaps are standing next to each other.

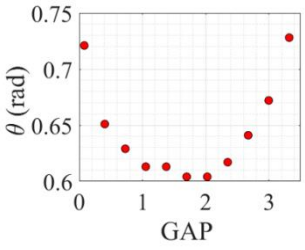

GAP	Max	RMS
0.08	0.721	0.646
1.70	0.604	0.531
3.32	0.728	0.647

Figure 5: RELATION BETWEEN THE GAP AS NONDIMENSIONAL SCALE OF FLAP'S WIDTH AND THE MAXIMUM RESPONSE

As previously explained, this study limited the lower and upper bound of the distances between the flaps in the channel. Therefore, the results presented in **Figure 5** show the maximum response according to the estimation of responses in the specified range of distances.

The interaction of the flaps is mostly affected by the presence of the confined water between the flaps and the breakwater.

The waves generated by the movement of flaps return back from the breakwater; therefore there is a continuous interaction between flaps and surrounding fluid.

In previous studies by means of numerical and experimental simulation has been shown that free oscillation of even one flap can cause other flaps to move [9], [17]. Therefore, it was expected that even by setting up flaps in each corner of the flume, some interaction effects between them can be seen.

The minimum of the peak is estimated for the distance equal to 1.70 times the flap width which is almost 20% less than the maximum response when the flaps are standing in the edges of the flume. The Root Mean Square (RMS) of the responses also follows the same pattern.

Moreover, the results are compared with the time series responses of a single flap oscillating in the middle of the flume.

The maximum response of flaps working an array of two in comparison with a single flap has an almost 0.8 % difference for gaps equal to 1.70 (see **Figure 6**).

Setting up flaps in each corner, the maximum gap, can increase the response to 21% in comparison to the single flap oscillation.

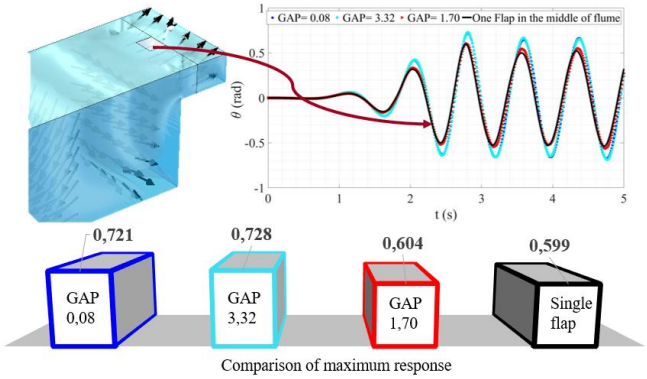

Figure 6: COMPARISON OF THE TIME SERIES RESPONSE OF ONE FLAP IN THE MIDDLE OF FLUME WITH AN ARRAY OF TWO FLAPS

In the graph, the response of two limits of lower and upper gap equal to 0.08 and 3.32 are presented next to each other.

To investigate the effect of the number of flaps (five or two) in an array the results of a two flap array in the maximum distance are also compared with the response of the five flaps array (see **Figure 7**).

As was previously shown in **Figure 1**, when there are five flaps mounted on the breakwater, the gap between the flaps is 0.08 of the flap's width.

The difference between the maximum rotation of these two arrays can be related to the period of a flap in an array of five or two. From the time series responses, the period of a flap oscillating in an array of two is almost 3 % less than a period of flap oscillating in a five flap array. The interaction between the flaps and the confined water was previously investigated in [18].

From the previous study [18], it was found that the transient response is damped out nearly in the first two cycles, and the response amplitude would be the same for the further cycles. Therefore, for the sake of brevity, only primary cycles of the response are presented here.

Despite the increase of response of five flaps in the first cycle of transient response, the time-series response of an array of two flaps shows more rotation than five flaps.

It should be emphasized that the response of flaps in an array of five have the same phase and almost the same amplitude; which causes the response time-series of Flap 1 to 5 to overlap each other.

To investigate the effect of PTO on the response, both the time-series response with and without PTO are represented. As expected, the amplitude of oscillation without the presence of PTO shows the higher values; however, the percentage difference with and without PTO effects is roughly the same.The power extracted from a flap oscillating in an array of flaps for

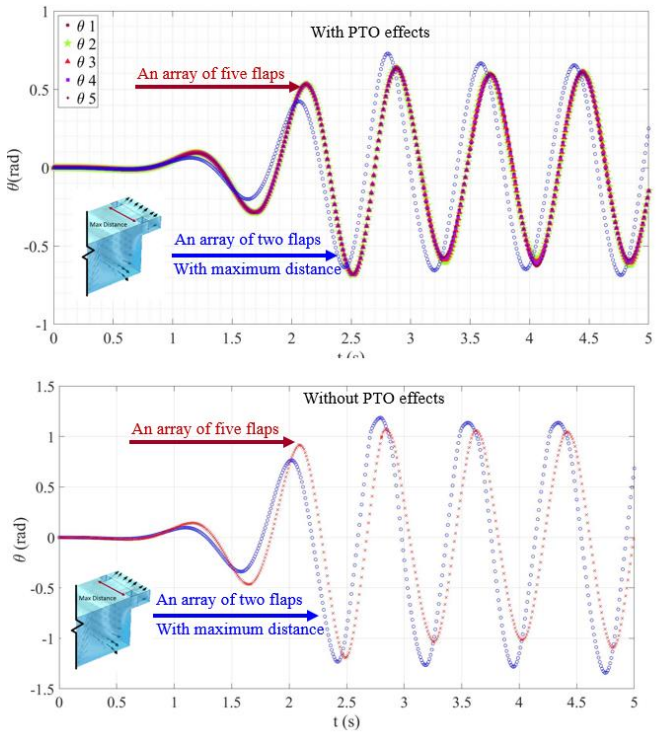

Figure 7: TIME SERIES RESPONSES FOR AN ARRAY OF FIVE FLAPS IN COMPARISON WITH AN ARRAY OF TWO FLAPS: WITH PTO EFFECTS (TOP); WITHOUT PTO EFEFCTS (BOTTOM)

the maximum distance is calculated from the formula $\frac{1}{T_w}\int_0^{T_w} C_P\dot{\theta}^2 dt$ over a wave period T_w [16], [26].

C_P is the PTO damping and $\dot{\theta}$ is the flap velocity. The time-series power is presented in **Figure 8**. Although some differences in the amplitude and phase of the power are observed; a flap working in an array of two, has higher oscillation.

By vanishing the transient response, the power amplitude of flaps oscillating in an array of five and an array of two almost becomes similar. The maximum difference in their amplitude reached less than 2% at time intervals of 5s to 6 s (see **Figure 8**).

By implying PTO effects, the oscillation of flaps operating in different arrays changed which caused the average power to remain the same. The average power for the first six seconds for a flap working in both arrays has the same value with a maximum 1% difference.

It can be seen that the maximum power in array of five at time 1.9 s and 2.4 s are followed by the maximum in array of two in 2.9 s and 3.8 s which makes nearby average for a flap working in both arrays.

It was previously mentioned that the response of all flaps in an array of five or two to this wave characteristics have the same pattern in terms of amplitude and period. Therefore, the times

series responses of all flaps overlapped each other as was shown in **Figure 7**- Top.

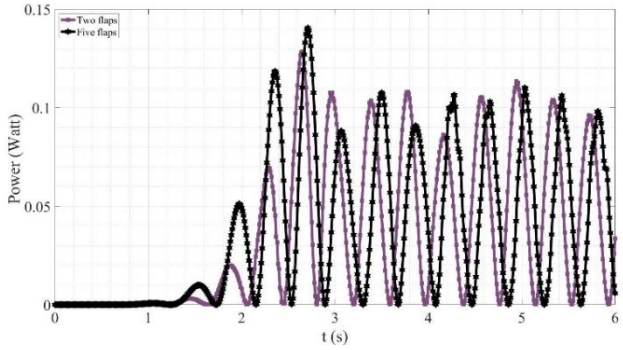

Figure 8: POWER TIME-SERIES FOR A FLAP OSCILLATING IN AN ARRAY OF TWO AND AN ARRAY OF FIVE FLAPS

3.2 Two flaps with different dynamic characteristics

In Section 3.1, the dynamic characteristics of the flap remains the same in a way that make the flap natural period near the half of the incoming wave period, 0.78 s.

Here, for each set of analyses, the mass of the flap is changed and by a code developed in Matlab [27], the moment of inertia and hydrostatic stiffness is calculated and used for the numerical simulation.

In this study, one flap mass is set to make a flap have a natural period equal, half and twice the incoming wave period, the other flap will have the natural period equal to the half of the incoming wave period.

The reason for selecting this combination is to use the different possible resonances that would happen when the period of the incoming wave is equal, multiple, or fraction of the natural period of the structure [28].

In this part, the PTO effects are ignored. Since the PTO coefficients found in the previous study were tuned for the specific Flap with the half period. Thus, the focus is on the flap's response which is previously shown that the amplitude of the response and the extracted power are connected [18], [28], [29].

Figure 9 shows the time-series response, maximum, and RMS for an array of two flaps in the maximum distance (edge of the flume) and with similar and different dynamic characteristics. The flaps are named F1 and F5, the corresponding period of Flaps are also named T1 and T5.

Since the natural period is one of the generally accepted representations of the dynamic behavior of the structure e.g. [30], in the graphs the diversity of dynamic characteristics is shown by natural periods.

Here, it can be seen that by changing the dynamic characteristics, the flaps can oscillate differently.

From the response, two flaps with different periods one with half and another with almost equal to the incoming wave period can make the maximum response in both flaps.

Although the difference is near 2 % from the flaps with equal periods, it is expected that the difference can be increased for flaps in open sea. This can be explained by the effect of the interaction of the waves behind the flaps in the confined water which synchronize the movement of flaps to one another.

T1(s)	T5(s)	Max_F1 (rad)	Max_F5 (rad)	RMS_F1 (rad)	RMS_F5 (rad)
0.373	0.373	1.186	1.188	1.059	1.057
0.805	0.373	1.156	1.195	1.081	1.06
1.558	0.373	1.041	1.206	0.945	1.079

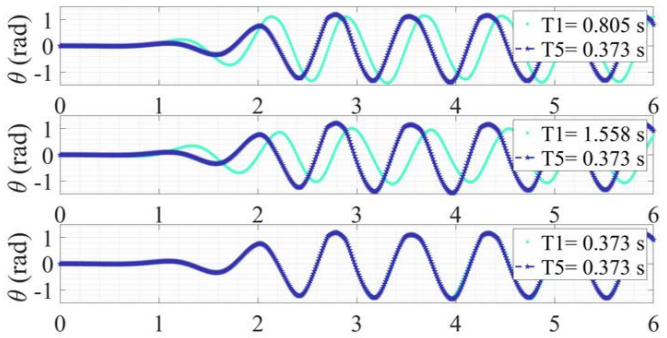

Figure 9: TIME-SERIES RESPONSES OF FLAPS IN AN ARRAY OF TWO WITH DIFFERENT DYNAMIC CHARACTERISITCS AND MAXIMUM GAP

3.3 Five flaps with different dynamic characteristics

The findings from the previous section for an array of two flaps are further studied for five flaps. The time-series response for flaps with the same and different dynamic characteristics are presented in **Figure 10**.

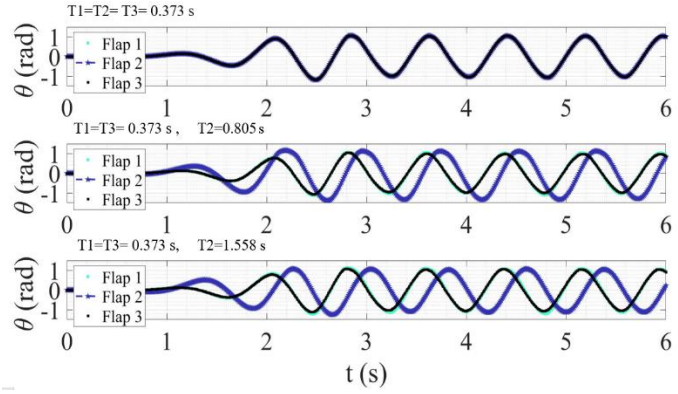

Figure 10: TIME-SERIES RESPONSES OF FLAPS IN AN ARRAY OF FIVE WITH DIFFERENT DYNAMIC CHARACTERISITCS

Due to the symmetry and for increasing the clarity of the graphs, only time-series responses of three flaps in an array of five are represented in **Figure 10**.

The response of a combination of flaps with a period equal to or half of the incoming wave period is increased in comparison to the array with similar dynamic characteristics. As it is shown

by the natural period of the flaps, the dynamic characteristics for any two near flaps are not the same.

It is expected that the increase of the response and interaction of the flaps shows itself much more if the flaps are not placed on a breakwater. Since the presence of the breakwater and interaction of waves, increase the tendency of flaps to move together.

The presence of breakwater has an advantage as its reflected wall properties can increase the response for flaps with similar tuned dynamic characteristics. However, to extract more power considering the variability waves and uncertainty involved; flaps with various natural periods corresponding to most dominant predefined wave characteristics (not only one wave) can increase the chance of steady power extraction in due time.

The results for two flaps with different dynamic characteristics in an array of two and five are summarized as matrix form in **Figure 11**.

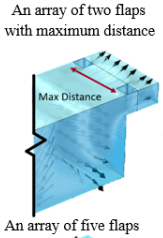

T1 (s)	T5 (s)	Max_F1 (rad)	Max_F5 (rad)
0.373	0.373	1.186	1.188
0.805	0.373	1.156	1.195
1.558	0.373	1.041	1.206

T2 (s)	T5 (s) T1 (s)	Max_F2 (rad)	Max_F5 (rad) Max_F1 (rad)
0.373	0.373	1.064	1.069
0.805	0.373	1.161	1.067
1.558	0.373	1.072	1.131

Figure 11: MATRIX FORM SUMMARY OF THE EFFECTS OF DYNAMIC CHARACTERISTICS ON FLAP'S RESPONSE IN AN ARRAY OF TWO AND FIVE

4. CONCLUSION

A trend of the Parabolic curve is discovered for the response of the flaps with their distances in a farm, which indicates a nearly 20 % difference in the maximum and RMS amplitude.

The moment of inertia and hydrostatic stiffness of the flaps in an array of two and five are changed and their effects on the response were investigated. The natural period has been chosen as the representative of dynamic characteristics' change.

It was found that the most efficient ratio of dynamic characteristics in an array of two is having a period half to the incoming wave period. For an array of five, the staggered layout of flaps with period half and equal to the incoming wave period 4% increase the overall response of each flap.

Here the combination of equal to or half or twice of one incoming wave period has been used. However, this idea can be utilized for making flaps with different natural periods near the dominant wave periods in an array.

Therefore, it can be generally suggested that by using flaps that each one will experience resonance to different waves; the steady maximum power extraction can be guaranteed. On the other hand, changing the distance between flaps can lead to the amplification of the response and can be transmited to the others.

This is the subject of the future study, to investigate the power of flaps with different dynamic characteristics to dominant waves in the open sea to study the influence of the real boundary conditions on the flap response and consequently the power absorption.

ACKNOWLEDGEMENTS

This work is part of the Verification through Accelerated testing Leading to Improved wave energy Designs (VALID) project. This project has received funding from the European Union's Horizon 2020 research and innovation programme under grant agreement No 101006927.

REFERENCES

[1] B. Howey *et al.*, "Compact floating wave energy converter arrays: Inter-device mooring connectivity and performance," *Appl. Ocean Res.*, vol. 115, no. August, 2021, doi: 10.1016/j.apor.2021.102820.

[2] A. Babarit, "On the park effect in arrays of oscillating wave energy converters," *Renew. Energy*, vol. 58, pp. 68–78, 2013, doi: 10.1016/j.renene.2013.03.008.

[3] S. H. Yang, J. W. Ringsberg, and E. Johnson, "Wave energy converters in array configurations—Influence of interaction effects on the power performance and fatigue of mooring lines," *Ocean Eng.*, vol. 211, no. August 2019, p. 107294, 2020, doi: 10.1016/j.oceaneng.2020.107294.

[4] P. Balitsky, G. Verao Fernandez, V. Stratigaki, and P. Troch, "Assessing the Impact on Power Production of WEC array separation distance in a wave farm using one-way coupling of a BEM solver and a wave propagation model," *Proc. 12th Eur. Wave Tidal Energy Conf. Cork, Irel.*, no. September, p. {1176\hyphen 1}--{1176\hyphen 10}, 2017.

[5] F. X. Correia da Fonseca, R. P. F. Gomes, J. C. C. Henriques, L. M. C. Gato, and A. F. O. Falcão, "Model testing of an oscillating water column spar-buoy wave energy converter isolated and in array: Motions and mooring forces," *Energy*, vol. 112, pp. 1207–1218, 2016, doi: 10.1016/j.energy.2016.07.007.

[6] C. Fitzgerald and G. Thomas, "A preliminary study on the optimal formation of an array of wave power devices," Sep. 2007.

[7] Y. Wei *et al.*, "Frequency-domain hydrodynamic

modelling of dense and sparse arrays of wave energy converters," *Renew. Energy*, vol. 135, pp. 775–788, 2019, doi: 10.1016/j.renene.2018.12.022.
[8] M. Murai, Q. Li, and J. Funada, "Study on power generation of single Point Absorber Wave Energy Converters (PA-WECs) and arrays of PA-WECs," *Renew. Energy*, vol. 164, pp. 1121–1132, 2021, doi: 10.1016/j.renene.2020.08.124.
[9] S. Saeidtehrani, "Physical and numerical modeling of a wave energy converter (PhD Thesis)," Roma Tre University, 2016.
[10] F. Kara, "Time domain prediction of power absorption from ocean waves with wave energy converter arrays," *Renew. Energy*, vol. 92, pp. 30–46, 2016, doi: 10.1016/j.renene.2016.01.088.
[11] P. Rosa-Santos *et al.*, "Experimental study of a hybrid wave energy converter integrated in a harbor breakwater," *J. Mar. Sci. Eng.*, vol. 7, no. 2, pp. 1–18, 2019, doi: 10.3390/jmse7020033.
[12] X. L. Zhao, D. Z. Ning, Q. P. Zou, D. S. Qiao, and S. Q. Cai, "Hybrid floating breakwater-WEC system: A review," *Ocean Eng.*, vol. 186, no. June, p. 106126, 2019, doi: 10.1016/j.oceaneng.2019.106126.
[13] P. Sammarco, S. Michele, and M. D'Errico, "Il cassone syncres: assorbimento del moto ondoso e generazione di energia elettrica," Rome, Italy, 2015.
[14] P. Sammarco, S. Michele, and M. d'Errico, "Flap gate farm: From Venice lagoon defense to resonating wave energy production. Part 1: Natural modes," *Appl. Ocean Res.*, vol. 43, pp. 206–213, 2013, doi: 10.1016/j.apor.2013.10.001.
[15] C. Mei, M. Stiassnie, and D. Yue, *Theory and applications of ocean surface waves. Part I: Linear aspects*. World Scientific, 2005.
[16] G. B. E. Renzi, A. Abdolali and F. Dias, "Mathematical modelling of the oscillating wave surge converter," 2012.
[17] S. Saeidtehrani, "Flap-type wave energy converter arrays: nonlinear dynamic analysis," *Ocean Eng.*, vol. 236, 2021, [Online]. Available: https://doi.org/10.1016/j.oceaneng.2021.109463.
[18] S. Saeidtehrani and M. Karimirad, "Multipurpose breakwater: Hydrodynamic analysis of flap-type wave energy converter array integrated to a breakwater," *Ocean Eng.*, vol. 235, p. 109426, 2021, doi: https://doi.org/10.1016/j.oceaneng.2021.109426.
[19] I. A. Svendsen, *Introduction to Nearshore Hydrodynamics*, vol. 24. World Scientific, 2006.
[20] J. Jia, *Essentials of Applied Dynamic Analysis*. Springer, 2014.
[21] D. Anderson, J. C. Tannehill, and R. H. Pletcher, *Computational fluid mechanics and heat transfer*. CRC Press, 2016.
[22] A. G. Alenitsyn, E. I. Butikov, and A. S. Kondratyev, *Concise Handbook of Mathematics and Physics*. Taylor & Francis, 1997.
[23] E. I. Butikov, "Parametric Resonance," *Comput. Sci. Eng.*, vol. 1, no. 3, pp. 76–83, 1999, doi: 10.1109/5992.764219.
[24] A. H. Nayfeh and D. T. Mook, *Nonlinear Oscillations*. Wiley, 1979.
[25] Paolo Sammarco, Simone Michele, Michele d'Errico, and G. Bellotti, "IL CASSONE SYNC.RE.S," 2016.
[26] M. Folley, Ed., *Numerical Modelling of Wave Energy Converters*. Elsevier Inc., 2016.
[27] "Matlab," 2020. www.mathworks.com.
[28] S. Saeidtehrani, P. Lomonaco, A. Hagmuller, and M. Levites-ginsburg, "Application of a simulation model for a heave type wave energy converter," *Proc. Twelfth Eur. Wave Tidal Energy Conf.*, pp. 948_1-948_8, 2017.
[29] S. Saeidtehrani, "Study on hydrodynamic characteristics and efficiency of a prototype wave energy converter," in *Proceedings of the Fourteenth European Wave and Tidal Energy Conference*, 2021, pp. 2065_1--2065_ 8.
[30] R. W. Clough and J. Penzien, *Dynamics of Structures*. McGraw-Hill, 1993.